

## Supplementary Information for

# Identification of potential aggregation hotspots on A $\beta$ 42 fibrils blocked by the anti-amyloid chaperone-like BRICHOS domain

Rakesh Kumar<sup>1</sup>, Tanguy Le Marchand<sup>2</sup>, Laurène Adam<sup>1</sup>, Raitis Bobrovs<sup>3</sup>, Gefei Chen<sup>1</sup>, Jēkabs Fridmanis<sup>3</sup>, Nina Kronqvist<sup>1</sup>, Henrik Biverstål<sup>1</sup>, Kristaps Jaudzems<sup>3</sup>, Jan Johansson<sup>1</sup>, Guido Pintacuda<sup>2</sup>, Axel Abelein<sup>1,\*</sup>

<sup>1</sup> Department of Biosciences and Nutrition, Karolinska Institutet, 141 83 Huddinge, Sweden

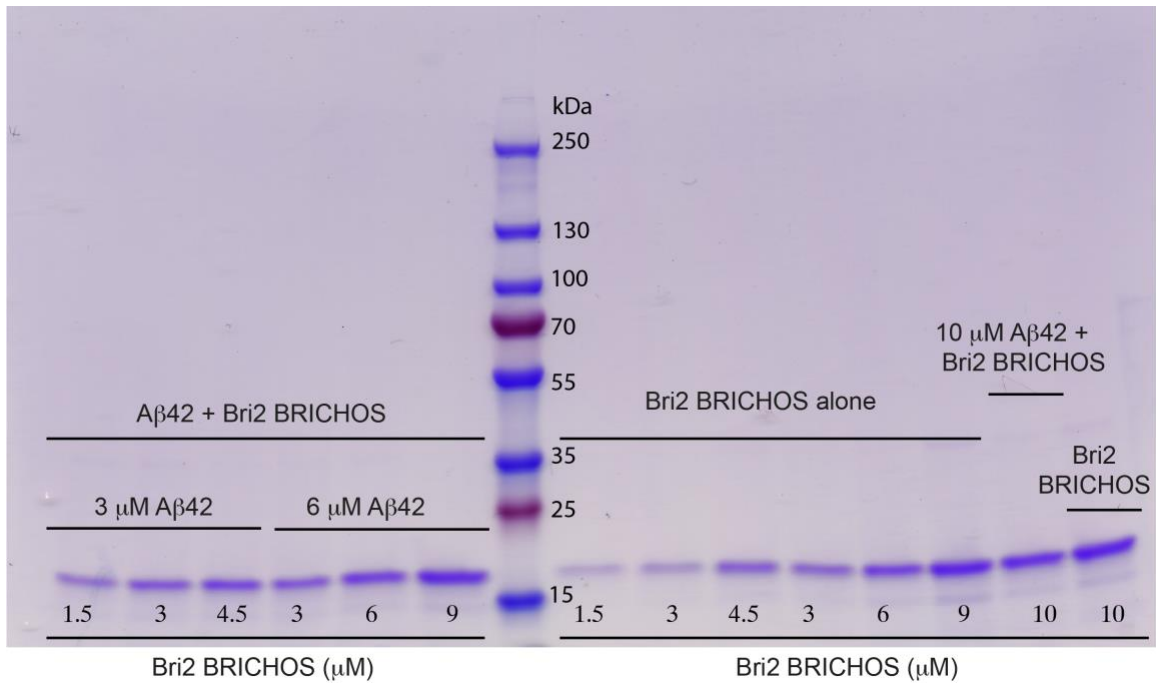
<sup>2</sup> Université de Lyon, Centre de Résonance Magnétique Nucléaire (CRMN) à Très Hauts Champs de Lyon (UMR 5082 - CNRS, ENS Lyon, UCB Lyon 1), 69100 Villeurbanne, France

<sup>3</sup> Department of Physical Organic Chemistry, Latvian Institute of Organic Synthesis, Riga, Latvia

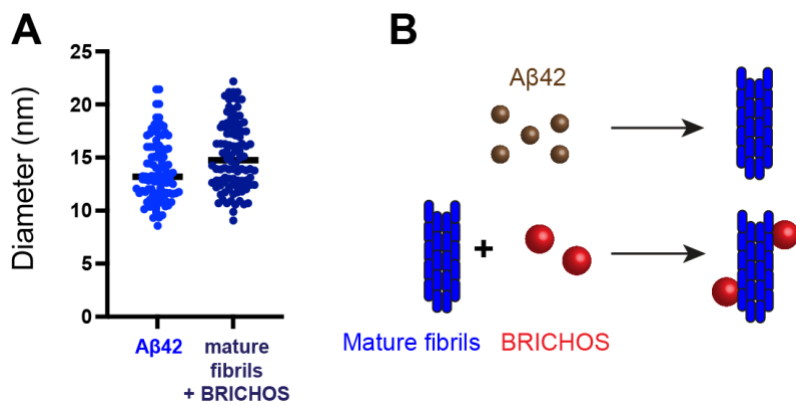
\*corresponding author: Axel Abelein

**Email:** axel.abelein@ki.se

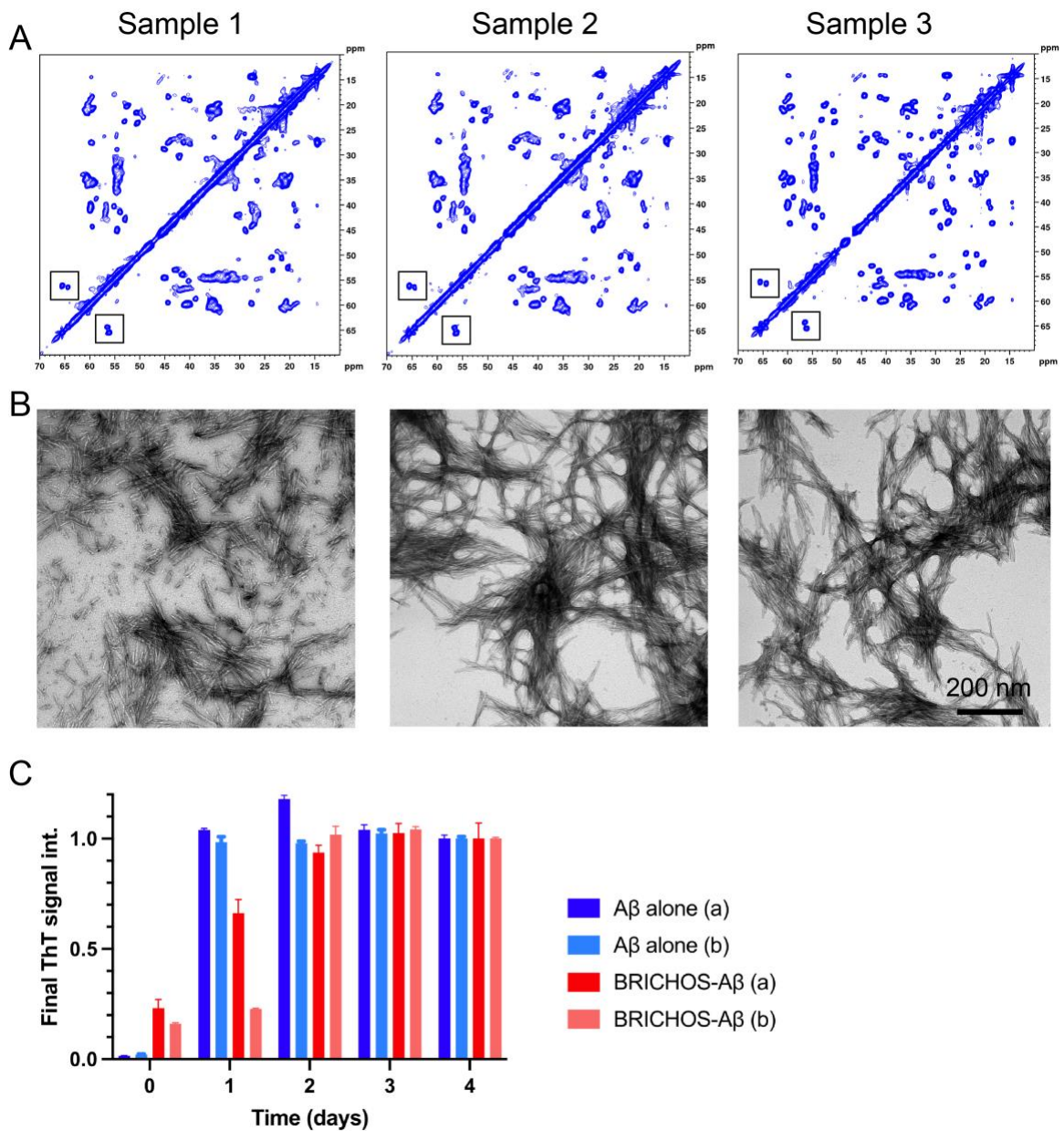
## Supplementary Information Figures



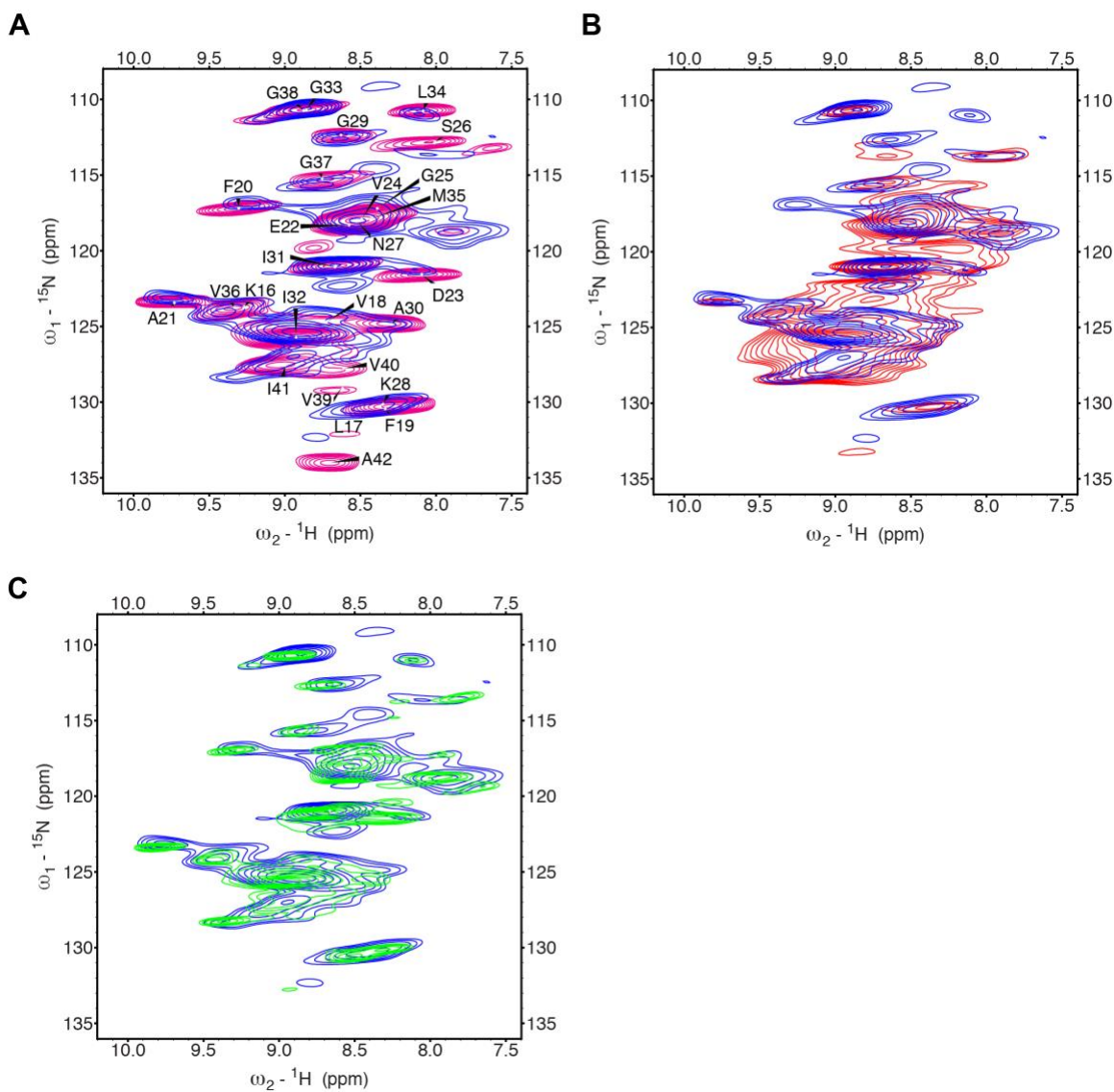
**Supplementary Figure 1. SDS-PAGE analysis of BRICHOS binding to A $\beta$ 42 fibrils – uncropped SDS-PAGE gel of Figure 1C.** Different concentrations of BRICHOS (1.5 to 10  $\mu$ M) were co-incubated with different concentrations of A $\beta$ 42 (3, 6 and 10  $\mu$ M) to form fibrils. The samples were centrifuged and the supernatant loaded on the SDS-PAGE gel. The results show that most BRICHOS is still in the supernatant and not bound to the fibrils. The last two lanes are shown in Figure 1C.



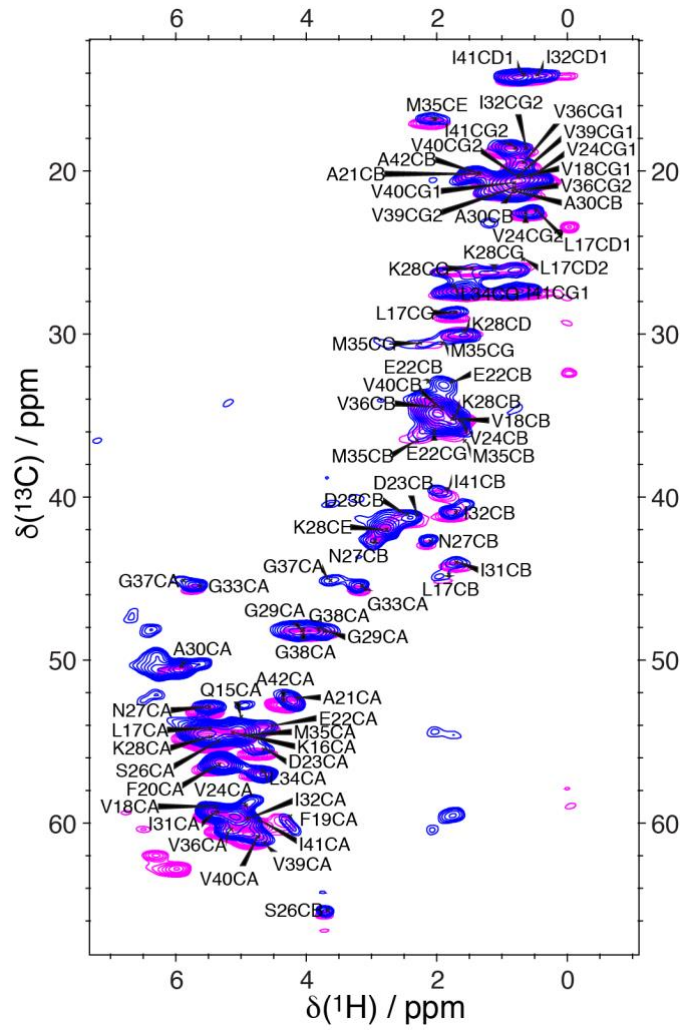
**Supplementary Figure 2. Fibril diameter of BRICHOS added to mature Aβ42 fibrils. (A)** Analysis of fibril diameters of mature Aβ fibrils with and without added BRICHOS reveals very similar values. n=100 independent measurements are shown where the line corresponds to the mean. Source data are provided as Source Data file. **(B)** Schematic overview about sample preparation.



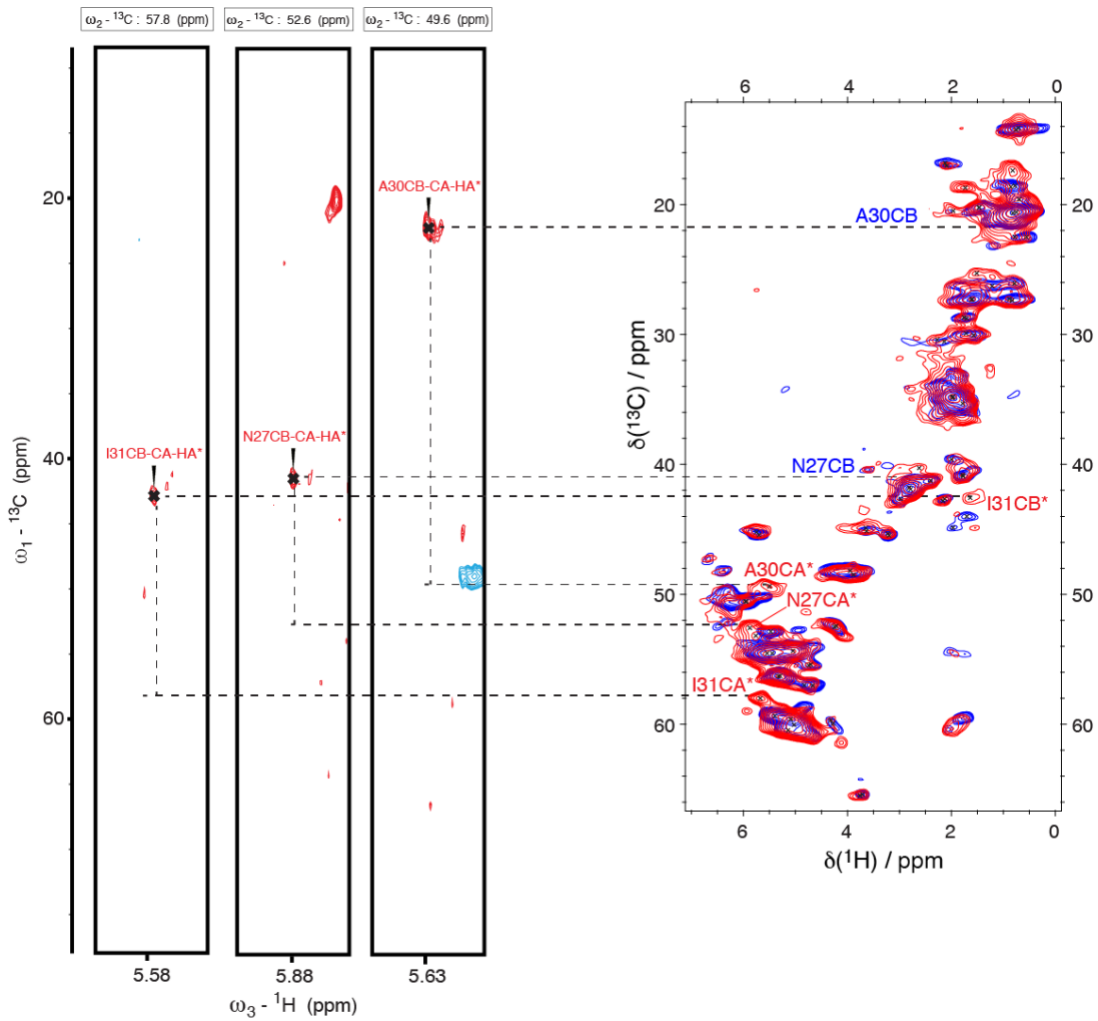
**Supplementary Figure 3.  $^{13}\text{C}$ - $^{13}\text{C}$  DARR spectra, EM images of different sample preparations for A $\beta$ 42 alone fibrils and final ThT signal intensity. (A)**  $^{13}\text{C}$ - $^{13}\text{C}$  DARR spectra and **(B)** EM images of different sample preparations as described in Supplementary Table 2. Sample 3 exhibits the sharpest signals and the two distinct peaks at around 55-60 ppm correspond to the two serine signals (marked in the box), indicating one major fibril morphology. **(C)** Final ThT intensities of A $\beta$ 42 alone and BRICHOS-A $\beta$ 42 co-incubated samples at different time points. The samples were incubated in the same manner as used for the preparation of the ssNMR samples, where small aliquots were taken and the ThT intensity was measured in a ThT plate using four replicates. The individual errors represent the standard derivations of these four replicates and the experiment was repeated twice, referred to as (a) and (b).



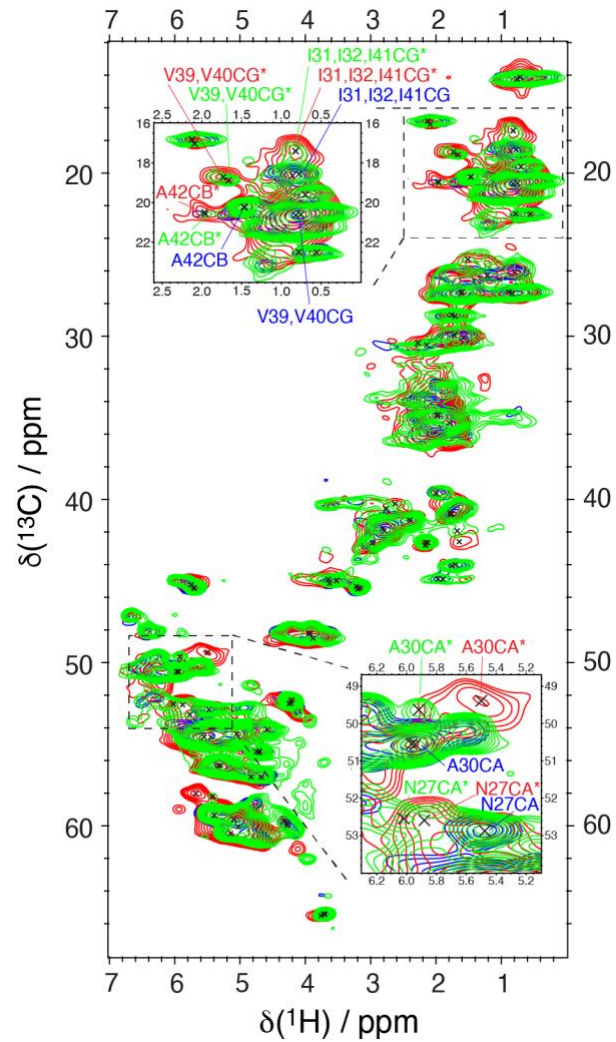
**Supplementary Figure 4.  $^1\text{H}$ ,  $^{15}\text{N}$ -correlation spectra of A $\beta$ 42 fibrils and the effect of BRICHOS. (A)**  $^1\text{H}$ ,  $^{15}\text{N}$ -correlation spectra of A $\beta$ 42 fibrils alone (blue) overlaid with the spectrum and assignment as published by Griffin & coworkers (pink) <sup>1</sup>. **(B,C)** Overlap of  $^1\text{H}$ ,  $^{15}\text{N}$ -correlation spectra of A $\beta$ 42 fibrils alone (blue) with (B) BRICHOS-A $\beta$ 42 co-incubated fibrils (red) and (C) BRICHOS added to mature A $\beta$ 42 fibrils (green).



**Supplementary Figure 5.**  $^1\text{H}$ ,  $^{13}\text{C}$ -correlation spectra of A $\beta$ 42 fibrils. Comparison of A $\beta$ 42 fibrils recorded here (blue) with the published spectrum and assignment of Griffin & coworkers (pink) <sup>1</sup>.

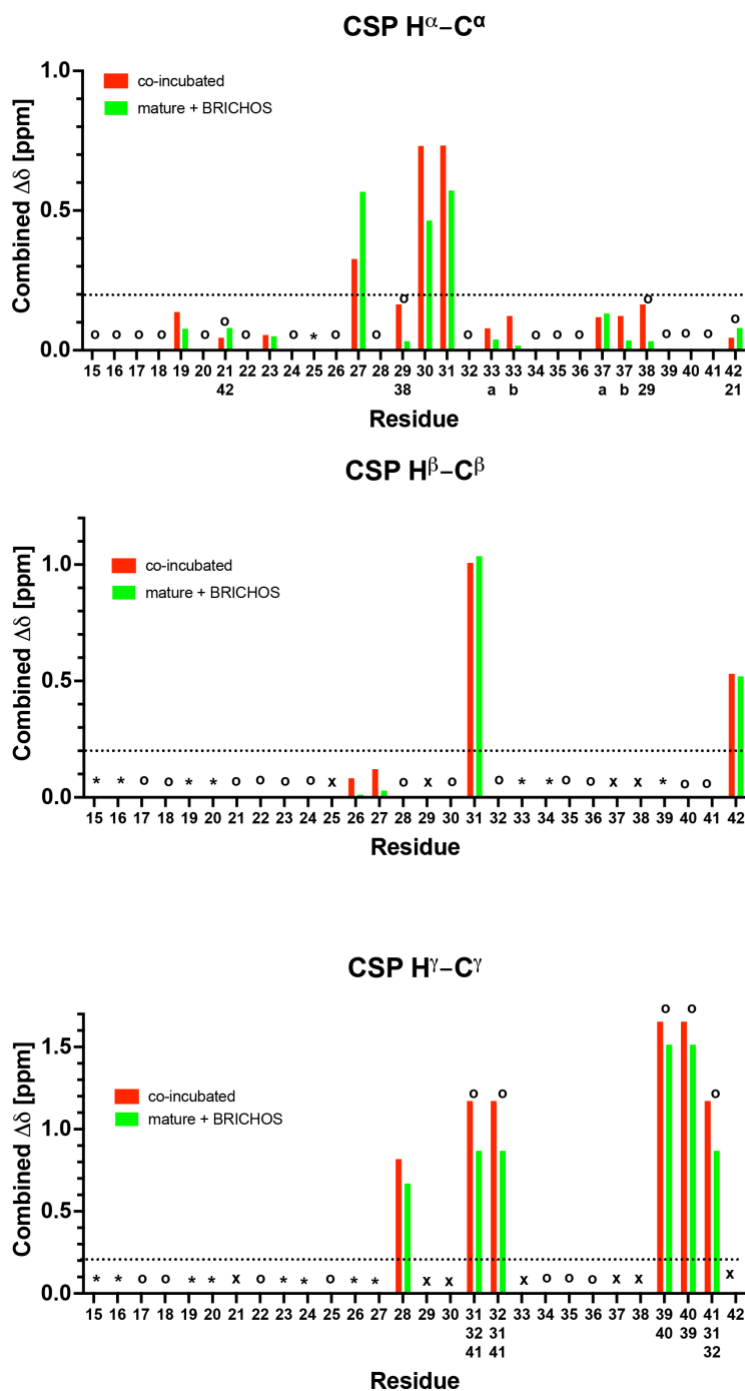


**Supplementary Figure 6. Assignment of shifted peaks of BRICHOS-A $\beta$ 42 fibrils using (H)CBCAH experiment.** Spectra are shown for A $\beta$ 42 fibrils alone (blue) and BRICHOS-A $\beta$ 42 fibrils (red). Strips of (H)CBCAH experiment of the three doubled peaks, marked with a star, in the CA-region using previous assignment of A $\beta$ 42 alone fibrils <sup>1</sup>.



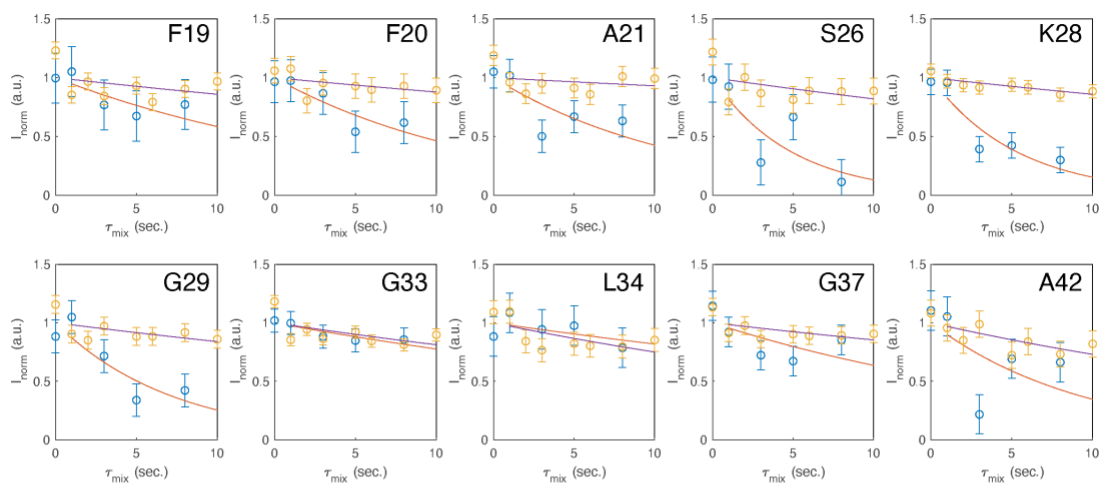
**Supplementary Figure 7.  $^1\text{H}$ ,  $^{13}\text{C}$ -correlation spectra.** The  $^1\text{H}$ ,  $^{13}\text{C}$ -correlation spectra of A $\beta$ 42 fibrils alone (blue), BRICHOS added to mature A $\beta$ 42 fibrils (green) and BRICHOS-A $\beta$ 42 co-incubated samples (red) are shown. The inserts represent different zoomed regions. The assignments of the doubled peaks visible in the BRICHOS samples are marked with a star (\*).



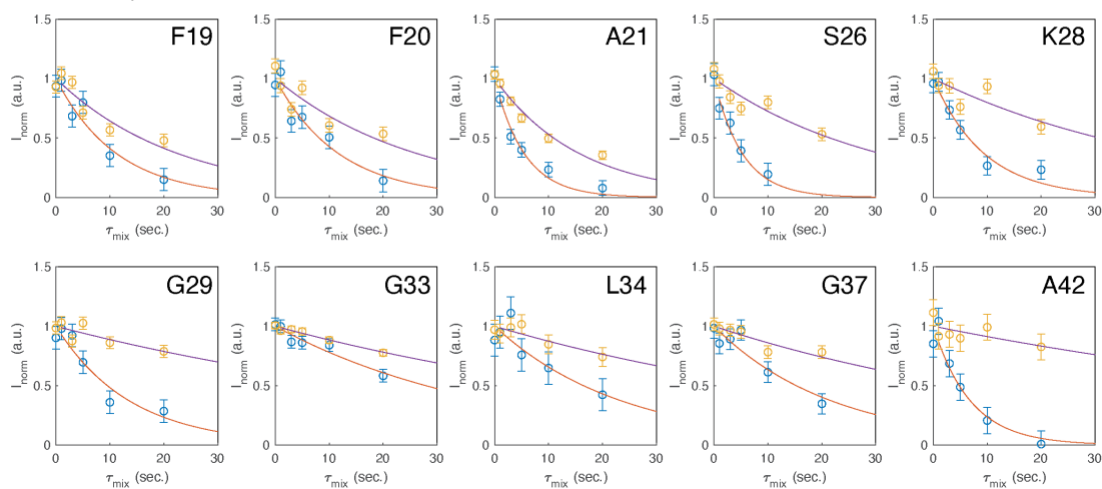


**Supplementary Figure 8. Chemical shift differences between doubled peaks in  $^1\text{H}$ ,  $^{13}\text{C}$ -correlation spectra.** Combined ( $^1\text{H}$  and  $^{13}\text{C}$ ) chemical shift changes between the set of signals of mature A $\beta$ 42 fibrils alone and the new set of peaks visible in co-incubated BRICHOS-A $\beta$ 42 fibrils (red) and those visible in BRICHOS added to mature A $\beta$ 42 fibrils (green). Due to the low intensity of the doubled peaks of the BRICHOS added to mature A $\beta$ 42 fibrils samples, these peaks were assigned based on the doubled peaks of the co-incubated BRICHOS-A $\beta$ 42 fibril sample. Missing assignments are labeled with an asterisk (\*), crosses (x) refer to nuclei that are not present in the corresponding residue and overlaps are marked by circles (o) where ambiguous assignments for the residues are stated.

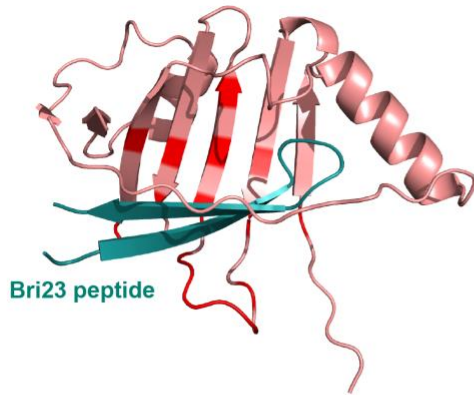
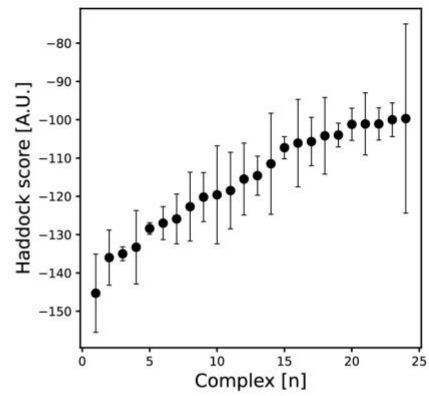
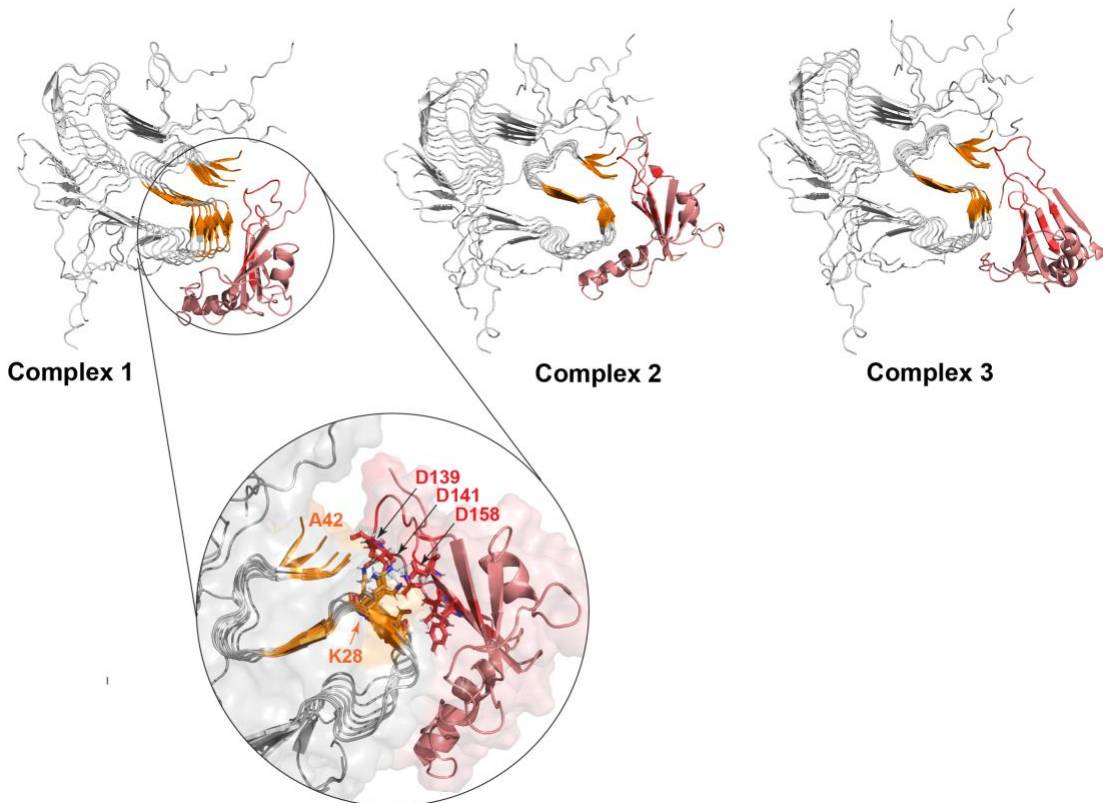
### A $^{15}\text{N}$ $R_1$ PRE Cu-EDTA A $\beta$ fibrils



### B $^{15}\text{N}$ $R_1$ PRE Cu-EDTA A $\beta$ fibrils in presence of BRICHOS



**Supplementary Figure 9. PRE effect of Cu-EDTA.** Longitudinal  $^{15}\text{N}$   $R_1$  relaxation rates and exponential fits for assigned residues in  $^1\text{H}$ ,  $^{15}\text{N}$ -correlation spectra of A $\beta$ 2 fibrils alone (A) and with BRICHOS added to mature A $\beta$ 2 fibrils (B), before (orange) and after (blue) of Cu-EDTA to determine the PRE effect of Cu-EDTA <sup>2,3,4</sup>.

**A Bri2 BRICHOS****B HADDOCK score****C Three best HADDOCK models**

**Supplementary Figure 10. HADDOCK models of BRICHOS-A $\beta$ 42 complexes.** (A) AlphaFold2 model of R221E Bri2 BRICHOS aligned with the Alpha2 model of full-length Bri2 protein where the natural amyloidogenic client, the Bri23 peptide, is shown. Residues close (within 5 Å) to Bri23 peptide are marked in red. (B) Haddock score of modeled complexes is presented. (C) The three best Haddock models are visualized where the interacting residues on A $\beta$ 42 fibril are marked in orange and on BRICHOS in red. The zoom-in graph shows the ionic interaction network between K28 on the A $\beta$ 42 fibril surface and D139, D141 and D158 of BRICHOS. MD models and the best HADDOCK complexes are provided as Supplementary data 1.

## Supplementary Information Tables

**Supplementary Table 1. Kinetic rate constants and apparent binding constants determined by SPR for BRICHOS binding to A $\beta$ 42 fibrils**

$k_{on,1}$ [ $M^{-1} s^{-1}$ ]	$k_{off,1}$ [ $s^{-1}$ ]	$k_{on,2}$ [ $M^{-1} s^{-1}$ ]	$k_{off,2}$ [ $s^{-1}$ ]	$K_{D1}$ [ $\mu M$ ]	$K_{D1}$ [nM]
$(3.61 \pm 0.03) \cdot 10^2$	$(6.69 \pm 0.04) \cdot 10^{-3}$	$(1.36 \pm 0.01) \cdot 10^4$	$(1.76 \pm 0.01) \cdot 10^{-4}$	$18.5 \pm 0.2$	$12.9 \pm 0.2$

**Supplementary Table 2. Conditions used for preparation of A $\beta$  fibril for ssNMR studies in the literature.**

Reference	Seeding	A $\beta$	[A $\beta$ ]	Shaking	Temp.	Buffer	Additives
Wälti et al., PNAS, 2016 <sup>5</sup>	10% for 3 generations	rec. 1-42	30 $\mu M$ (or 100 $\mu M$ )	350 rpm	37 °C	100mM NaP, pH 7.4	100 mM NaCl, 100 $\mu M$ ZnCl
Xiao et al., Nat Struc Mol Biol, 2015 <sup>6</sup>	5% for > 4 generations	syn. 1-42	50 $\mu M$	slowly agitated for 3-4d	RT	10mM NaP, pH 7.4	No
Colvin et al., JACS, 2016 <sup>7</sup>	no, simply incubated in Falcon tubes	rec. M1-42	10-50 $\mu M$	no	RT	20mM NaP, pH 8, 0.2mM EDTA, 0.02% NaN3	No

**Supplementary Table 3. Screening conditions for homogeneous production of A $\beta$ 42 fibrils alone.**

Samples	Seeding	A $\beta$	[A $\beta$ ]	Shaking	Temp.	Buffer	Additives
Sample 1	10% for 1 generations	rec. 1-42	30 $\mu M$	no	25 °C	20mM NaP, pH 8, 0.02% NaN3, 0.2mM EDTA,	No
Sample 2	10% for 4 generations	rec. 1-42	30 $\mu M$	no	25 °C	20mM NaP, pH 8, 0.02% NaN3, 0.2mM EDTA,	No
Sample 3	10% for 4 generations	rec. 1-42	30 $\mu M$	300-350 rpm	25 °C	20mM NaP, pH 8, 0.02% NaN3, 0.2mM EDTA,	No

**Supplementary Table 4. Transverse relaxation time  $T_2$  in ms of different fibril samples.**

Nucleus	Griffin et al.	A $\beta$ 42 alone	BRICHOS-A $\beta$ 42
<sup>1</sup> H	2.26	2.25	2.26
<sup>15</sup> N	68	66	49

## Supplementary References

1. Bahri S, *et al.* (1)H detection and dynamic nuclear polarization-enhanced NMR of Abeta1-42 fibrils. *Proc Natl Acad Sci U S A* **119**, (2022).
2. Öster C, *et al.* Characterization of Protein-Protein Interfaces in Large Complexes by Solid-State NMR Solvent Paramagnetic Relaxation Enhancements. *J Am Chem Soc* **139**, 12165-12174 (2017).
3. Aucoin D, *et al.* Protein-solvent interfaces in human Y145Stop prion protein amyloid fibrils probed by paramagnetic solid-state NMR spectroscopy. *J Struct Biol* **206**, 36-42 (2019).
4. Wickramasinghe NP, *et al.* Nanomole-scale protein solid-state NMR by breaking intrinsic 1HT1 boundaries. *Nat Methods* **6**, 215-218 (2009).
5. Wälti MA, *et al.* Atomic-resolution structure of a disease-relevant Abeta(1-42) amyloid fibril. *Proc Natl Acad Sci U S A* **113**, E4976-4984 (2016).
6. Xiao Y, *et al.* Abeta(1-42) fibril structure illuminates self-recognition and replication of amyloid in Alzheimer's disease. *Nat Struct Mol Biol* **22**, 499-505 (2015).
7. Colvin MT, *et al.* Atomic Resolution Structure of Monomorphic Abeta42 Amyloid Fibrils. *J Am Chem Soc* **138**, 9663-9674 (2016).